

# Three Dimensional Quantitative Myelin Water Imaging using Direct Visualization of Short Transverse Relaxation Time Component (ViSta)

Se-Hong Oh<sup>1,2</sup>, Sung Suk Oh<sup>2</sup>, Joon Yul Choi<sup>2</sup>, Jang-Yeon Park<sup>3</sup>, and Jongho Lee<sup>2</sup>

<sup>1</sup>Imaging Institute, Cleveland Clinic, Cleveland, Ohio, United States, <sup>2</sup>Department of Radiology, Perelman School of Medicine, University of Pennsylvania, Philadelphia, Pennsylvania, United States, <sup>3</sup>School of Biomedical Engineering, College of Biomedical and Health Science, Konkuk University, Chungju, Korea

**INTRODUCTION** Myelin water imaging (MWI) measures the signal from water molecules between myelin layers (1). This signal is characterized by a shorter  $T_2$  ( $T_2 < 40$  ms or  $T_2^* < 25$  ms at 3T) than other water (axonal/extracellular) signals. Recently, a new MWI method, Direct Visualization of Short Transverse Relaxation Time Component (ViSta (2); or background-suppressed MWI (3)), was proposed to acquire the myelin water signal based on the  $T_1$  difference among water pools. This method suppresses long  $T_1$  signals such that the remaining signal is from short  $T_1$  components, which have been suggested to originate from myelin water (4). When the signal characteristics of ViSta were explored, both  $T_2^*$  (2) and phase (5) showed similar characteristics to myelin water, suggesting that the ViSta signal is primarily from myelin water. Compared to conventional MWI, ViSta generates substantially improved myelin water images (Fig. 1), demonstrating feasibility for clinical applications. In this work, we 1) demonstrated that the ViSta signal shows short  $T_2^*$  characteristics (<25 ms) across the brain, 2) optimized the sequence and developed an efficient approach to acquire a 3D image of the whole brain and 3) suggested a way to quantify the myelin water fraction (MWF) in 3D ViSta.

**METHODS** Data were collected from five subjects in a 3T MRI scanner (IRB-approved).

**1) Characterization of  $T_2^*$  in multiple slices:** To verify the short  $T_2^*$  characteristics of ViSta across the brain, three slices, that do not overlap with a previously studied slice (2), were acquired using multi-echo 2D ViSta. The same scan parameters and analysis as in (2) were used to characterize the  $T_2^*$  spectrum. ROIs are shown in Figure 2.

**2) Development and optimization for 3D ViSta:** A computer simulation was performed to test the sensitivity of ViSta for RF timing and  $B_1$  inhomogeneity. The three timing intervals in ViSta ( $TI_1$ ,  $TI_2$ , and TD; Fig. 3) were jittered to test the effect of timing in long  $T_1$  suppression. The effects of transmit  $B_1$  inhomogeneity was also simulated. These results were incorporated into the design of the 3D ViSta sequence. For the sequence, a pair of adiabatic inversion RF pulses (hyperbolic secant; 10.24 ms, 1 kHz) was used to reduce  $B_1$  sensitivity and to suppress a wide range of long  $T_1$  signals ( $|M_{xy}|/M_0 < 0.25\%$  for  $750 < T_1 < 2000$  ms). The timing simulation suggested an increase in long  $T_1$  signal contribution for a few ms of timing errors. To minimize this sensitivity, the adiabatic inversion pulse was simulated to determine the inversion timing for a range of off-resonance spins. The results showed that spins are mostly inverted at 2 ms from the center of the inversion pulse (between  $-0.94M_0$  and  $-0.8M_0$  for  $|f_{off}| < 100$  Hz). The three intervals were adjusted accordingly (Fig. 3). For the excitation RF, no significant sensitivity to  $B_1$  was observed, and a SLR minimum phase excitation pulse (ref. 6; duration = 2.56 ms, TBW = 13.3) was designed to reduce the minimum TE so that the short  $T_2^*$  signal is acquired effectively. The echo time was reduced by 1.09 ms compared to a linear phase pulse of the same duration. The inflow of arterial blood, which resulted in artifacts, was reduced using a flow saturation pulse (300 ms from the first inversion pulse), which saturated a volume (= 11 cm) 5 mm below the imaging volume. Fat was saturated using an off-resonance saturation pulse. For the readout, a 3D segmented EPI was used. The scan parameters were as follows: 32 slices, FOV =  $240 \times 240 \times 128$  mm<sup>3</sup>, resolution =  $1.5 \times 1.5 \times 4$  mm<sup>3</sup>, TR/TE = 1160/6.5 ms,  $TI_1/TI_2/TD = 560/220/380$  ms, partial k-space in phase = 6/8, PE lines per segment = 11, number of segments = 11 and scan time = 6.53 min.

**3) Quantification:** For quantification, a proton density-weighted GRE sequence with the same readout as ViSta was acquired using a TR of 75 ms and flip angle of 5°. The scan time was 0.5 min. The ViSta data were divided by the GRE data and then scaled by the following factor:

$$\text{scale factor}(f) = k \cdot (\text{GRE } T_1\text{-weighting} \times \text{GRE } T_2^*\text{-weighting}) / (\text{ViSta } T_2^*\text{-weighting}) = k \left\{ \frac{(1 - \exp(-TR_G/T_{1,G})) \sin \theta_G}{[1 - \cos \theta_G \exp(-TR_G/T_{1,G})]} \cdot \exp(-TE_G/T_{2,G}^*) \right\} / (\exp(-TE_V/T_{2,V}^*))$$

where the subscript G (or V) represents the parameter of GRE (or ViSta):  $T_1$  of GRE = 800 ms,  $T_2^*$  of GRE = 50 ms, and  $T_2^*$  of ViSta = 10 ms. The constant,  $k$ , includes factors such as myelin water  $T_1$ -weighting, cross-relaxation, water exchange, and MT/direct saturation effects in ViSta. In this study,  $k$  only included the effects of myelin water  $T_1$ -weighting ( $T_1=118$  ms; ref.4).

**RESULTS** When the  $T_2^*$  spectra were investigated across the slices, all ROIs show that the signal is predominately from the short  $T_2^*$  in the range of myelin water (<25 ms; Table 1; shaded boxes are from ref. 2). This suggests that the ViSta signal is from myelin water throughout the brain. The computer simulation shows sensitivity to the  $B_1$  field in the inversion pulses (25%  $B_1$  variation may induce up to 18.8 times larger long  $T_1$  signals. For 5%  $B_1$  variation, it is up to 1.5 times). On the other hand, the variation in the excitation pulse has little effect. The short  $T_1$  signal ( $50 < T_1 < 200$  ms) shows less than 10% change when  $B_1$  variation is 25%. When the RF timing is tested, a 5 ms variation may increase a long  $T_1$  contribution up to 5.5 times. These potential compounds were carefully avoided in our ViSta sequences (2D and 3D) as described in Method. Figure 4 shows a quantitative 3D ViSta MWF map. It reveals higher MWFs in optic radiation, splenium, genu, internal capsule, and SLF and IFL areas. This map shows a similar 3D MWF distribution to a recent conventional MWI map using 3D GRASE (Fig. 4 in ref.

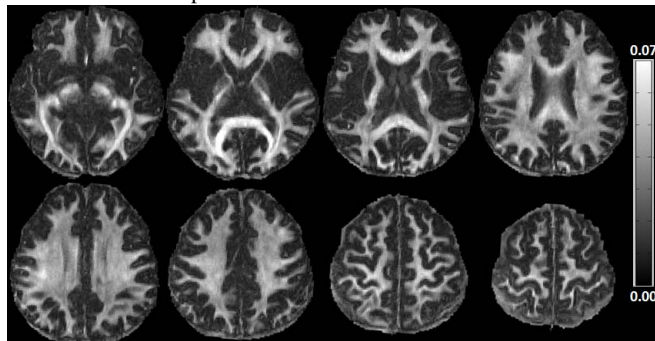


Figure 4 Quantitative 3D ViSta MWF map (8 out of 32 slices in 8 min.)

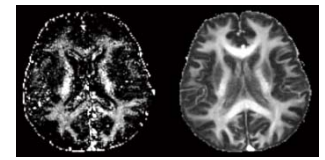


Figure 1 Conventional MWI (left) vs. ViSta (right)

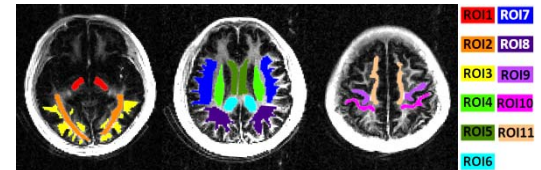


Figure 2. ROIs for  $T_2^*$  characterization

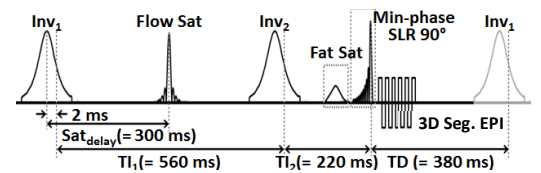


Figure 3. 3D segmented EPI ViSta sequence

	Relative to ViSta
ROI1	97.0 ± 1.5
ROI2	92.3 ± 2.2
ROI3	92.0 ± 2.0
ROI4	98.2 ± 1.3
ROI5	93.7 ± 3.4
ROI6	95.6 ± 0.9
ROI7	95.3 ± 1.0
ROI8	93.1 ± 1.0
ROI9	98.3 ± 1.0
ROI10	98.8 ± 0.8
ROI11	98.2 ± 1.0
Genu	100 ± 0.0
Splenium	91.4 ± 5.6
Maj. Forceps	95.2 ± 3.4
Min. Forceps	99.7 ± 0.6
Int. Capsule	99.6 ± 0.4
Mean	96.2 ± 2.9

Table 1

7). Compared to conventional MWI, the ViSta map illustrates superior image quality showing little or no speckle-like noise.

**DISCUSSION AND CONCLUSION** The new 3D ViSta sequence can cover a whole brain volume (FOV =  $240 \times 240 \times 128$  mm<sup>3</sup>, resolution =  $1.5 \times 1.5 \times 4$  mm<sup>3</sup>) in less than 8 min. and provide high quality myelin water images. Compared to conventional MWI, quantitative ViSta shows a smaller MWF due to incomplete knowledge of the constant ( $k$ ) in the scaling factor. Hence, ViSta MWF can be referred to as "apparent" MWF. However, the method can still be used for group comparisons or longitudinal studies as long as the same scaling factor is used.

**References:** [1] Mackay, 1994, MRM, 31, 673 [2] Oh, Neuroimage, 2013, 83C, 485 [3] Oh, ISMRM, 2013, #867 [4] Labadie, MRM, 2013, online [5] Kim, QSM 2<sup>nd</sup> workshop, 2013, #40 [6] Pauly, IEEE, 1991, 10, 53 [7] Prasloski, Neuroimage, 2013, 63, 533